UCRL-95314
PREPRINT

DESIGN OF EXTERNALLY PRESSURIZED GAS BEARINGS FOR STIFFNESS AND DAMPING

J. W. Roblee
Lawrence Livermore National Laboratory

C. D. Mote, Jr.
University of California

9th International Gas Bearing Symposium
National Bureau of Standards, Washington DC
September 8-10, 1986

September 5, 1986

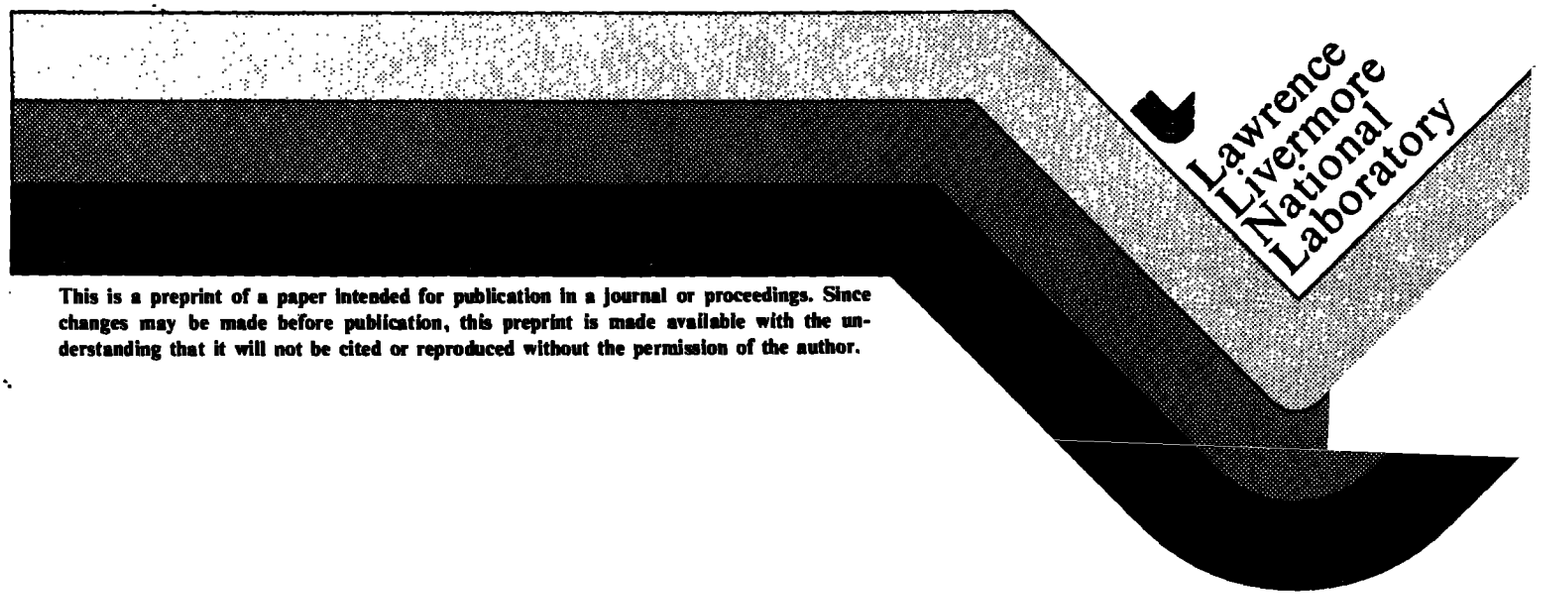

DESIGN OF EXTERNALLY PRESSURIZED GAS BEARINGS FOR STIFFNESS AND DAMPING

J. W. Roblee
Lawrence Livermore National Laboratory
Livermore, California

C. D. Mote, Jr.
University of California at Berkeley
Berkeley, California

ABSTRACT

A design method for flat, circular thrust bearings is presented in this paper. The design method is based upon a new dynamic model of the bearing and permits the selection of stiffness and damping for applications of bearings in vibrating environments. Application of the design method to the tuning of bearing dynamics is emphasized here, while the development of the dynamic model is discussed in other references. Design constraints are considered in the iterative design procedure and are illustrated in a bearing design example.

INTRODUCTION

In most gas bearing designs only the load, static stiffness, and flowrate of the externally pressurized gas are considered. So long as the bearing is stable, the frequency dependence of its dynamic stiffness is seldom considered. Some bearing design procedures do consider damping, but they give little guidance on how to make the most effective use of the limited damping in the bearing. Because externally pressurized gas bearings exhibit damping only over a narrow frequency band, they are often reputed to be poorly damped. In many applications, damping of machine vibrations is more important than the static stiffness of its bearings. Consequently, a compromise must be made between high static stiffness and the amount of damping in a gas bearing. The purpose of this paper is to present a bearing design procedure

that not only considers the load and flowrate requirements of the bearing, but tunes the dynamic stiffness of the bearing so that the dynamic response of the bearing-machine system is optimized. This design procedure utilizes a new dynamic model of gas bearings[1] that facilitates the tuning of its dynamic stiffness. Only a specific class of bearings is considered here, but the model has a wider range of applicability, and the design procedure can be generalized to other types of thrust bearings.

NOTATION

A_o	*Cross sectional area of the orifice
A_t	Total area of the bearing
C_d	Discharge coefficient of an orifice
f(s)	External dynamic force
H	*Steady state film thickness of the bearing
h(s)	Motion of the bearing about the steady state position
k	*Specific heat ratio of the gas
$K_b(s)$	Dynamic stiffness of the bearing
K_s	Static stiffness
K_∞	High-frequency stiffness ($K_b(\infty)$)
$\dot{M}$	Mass flowrate
M	Equivalent single degree of freedom mass
N	*Number of interior grooves
P_a	*Ambient pressure
P_r	Recess pressure
P_s	*Supply pressure
R	Gas constant in the perfect gas law
R_o	*Outer radius of the bearing
R_i	*Radius of the main recess grooves
s	Laplace variable
T	*Absolute temperature
V_r	*Gas volume in the recess grooves
w(s)	Dynamic component of the bearing load.
W	Bearing load
$\bar{\alpha}$	Stiffness Ratio (K_∞/K_s)
$\bar{\kappa}$	Dimensionless stiffness-to-mass ratio ($K_\infty \tau_1^2/M$)

ζ	Damping ratio
μ	*Kinematic viscosity
τ	Time constant of a pole or zero
ω	Frequency
Ψ	Bearing design parameter ($\mu^2 A_t^3/P_s M H^5$)

* A parameter needed to define a bearing design.

DEFINITION OF THE ABC CLASS OF BEARINGS

To demonstrate the utility of designing a bearing for stiffness and damping, a specific class of bearings is considered here. This class of bearing is of great practical interest, and it has a high dynamic stiffness which is amenable to tuning in the design process. The features of this class of bearing and the bearing's operational characteristics are listed below and will be described in more detail later in this paper. These operational characteristics are required to ensure the validity of the model used here, but this does not prevent an ABC bearing from operating at other conditions. For lack of a better term, this class of bearings will be denoted the ABC bearing in this paper. Its features are:

- o Flat
- o Circular
- o Externally pressurized with a gas
- o Compensated by low pressure drop orifices
- o Bearing film pressurized by grooves
- o Circular main feed groove
- o Large groove radius, implying a narrow perimeter region
- o Radial interior grooves
- o High supply pressure
- o Laminar flow in the film
- o Low sliding velocity
- o Small amplitude film thickness fluctuations

A MODEL OF THE DYNAMIC STIFFNESS OF THE ABC BEARING

Figure 1a illustrates the geometry of a typical, pocket thrust bearing and some of its key parameters, and Fig. 1b shows a grooved bearing of the ABC class. The parameters denoted by an asterisk in the Notation section completely define the ABC bearing. Gross[2] and many others (see the large bibliography in Ref. 1) discuss the pressure distribution in this type of bearing and its resulting load, flowrate, and static stiffness. The model used here makes similar assumptions and approximations, which are often valid in practice. The gas is assumed to obey the perfect gas law, to have constant viscosity, and to be isothermal in the gap separating the bearing surfaces. The flow in the bearing film is assumed to be subsonic and well into the laminar flow regime, as indicated by a modified Reynolds number[2] of $Re^* << 1$. To ensure that the entrance region of the film has a negligible effect on the pressure distribution, the perimeter region of the bearing must be sufficiently wide ($R_o - R_i > 200H$). The relative sliding velocity of the two bearing surfaces is also assumed to be small compared to the gas flow velocity. Finally, the gas is modeled as a continuum so the Reynolds equation[2] is valid, and the dynamic fluctuations of the film thickness (h(s)) are assumed to be small relative to the equilibrium film thickness (H) so the Reynolds equation can be linearized.

The static stiffness (K_s) of the ABC bearing is determined by the applied load (W), the gas flow through its orifice flow restrictor(s), and the laminar flow restriction in its perimeter region. At high frequencies of bearing oscillation, the gas within the bearing becomes trapped and acts as a pneumatic spring. The applied load (W), the recess volume (V_r) and the gap height (H) determine this high frequency limit to bearing stiffness. As shown in Gross[2], the bearing will be unstable if K_s exceeds the stiffness at high frequency. Therefore, the ABC bearings considered here are pressurized by recess grooves, similar to those shown in Fig. 1b, instead of a pocket. With grooves, the total recess volume is greatly reduced, and the same pressure distribution as a pocket bearing can be achieved. Circular bearings also minimize the length of the recess groove necessary to pressurize a given surface area. This recess groove can also be segmented and supplied by individual orifices to increase the bearing's stiffness for tilting moment

loads (Fig. 1b shows a main feed groove with three segments). In addition, a large interior region increases the stiffness and load carrying capacity of a bearing of specific size. Therefore, only bearings with a narrow perimeter region ($R_i > 0.7R_o$) are considered here.

The interior, radial grooves shown in Fig. 1b are used to alter the dynamic stiffness of the ABC bearing. When the bearing is oscillating under a dynamic excitation force, the gas in the interior behaves as a squeeze film[2], flowing into and out of the region. This gas flow is an additional source of bearing damping that can be tuned to operate in different frequency bands by varying the size of the sub-regions in the bearing interior. In the design procedure presented here, the size of the sub-regions is varied by changing the number of radial grooves and by varying the radius (R_i) of the main feed groove. Only three interior groove patterns - zero, three, or six grooves, each beginning at a radius of $0.2R_i$ - are considered here. Many other groove patterns are possible[1], but these three cases are sufficient for most design applications. The interior grooves do not significantly affect the steady state pressure distribution of the bearing because the gas in the interior region of the bearing is stagnant under steady state conditions. Since the interior grooves do not carry a steady flow of gas, they can have a much smaller cross section than the main recess groove supplying the bearing perimeter. Therefore, interior grooves produce only a small increase in the total recess volume (V_r) of the bearing.

A detailed derivation of the dynamic model of bearing stiffness used in this paper and its experimental verification are presented in Ref. 1. The model is derived to capture the dominant dynamic behavior of the ABC bearing. Consequently, it models the bearing stiffness well at low frequency and the majority of the bearing's damping at intermediate frequencies. However, the model does not capture the dynamic stiffness at very high frequencies, which are typically outside the range of interest for most design applications. The object of the model is to accurately predict the dominant pole and zero of the bearing's dynamic stiffness $K_b(s)$:

$$K_b(s) = \frac{w(s)}{-h(s)} = K_s \frac{(1+\tau_1 s)}{(1+\tau_2 s)} \quad , \tag{1}$$

where s is the Laplace variable. This pole and zero representation of the dynamic stiffness is convenient for design. The asymptotes of three possible stiffness amplitudes are shown in Fig. 2. The high frequency stiffness, represented by

$$K_\infty = \lim_{\omega \to \infty} K_b\ (j\omega) = \frac{\tau_1}{\tau_2} K_s \quad , \tag{2}$$

is the same for all three cases.

This analytical model of the dynamic stiffness was derived with a consistent set of approximations that acknowledges the uncertainties in the fabrication of a practical bearing. Consequently, the perimeter region and the orifice flow are represented simply by a linearized, lumped parameter model similar to that used by others[2]. However, the perimeter region model is coupled to an approximate, squeeze-film model of the interior region of the bearing[1]. At high frequencies, the perimeter region also behaves as a distributed parameter system, but for the narrow perimeter regions considered here, the departure from lumped parameter behavior is small. In this paper, the model is further restricted to highly stiff, well damped bearings. Therefore, only supply pressures (P_s) greater than three times ambient (P_a) and recess pressures (P_r) greater than $0.8P_s$ are considered. Lastly, only a gas specific heat ratio (k) of 1.4 is used here to reduce the number of variables.

TUNING THE DYNAMIC STIFFNESS OF THE ABC BEARING

The dynamic stiffness represented by Eqn. 1 and illustrated in Fig. 2 produces a positive phase shift between the frequencies $1/\tau_1$ and $1/\tau_2$, if $\tau_1 > \tau_2$. This shift produces a single frequency band with damping. As K_s approaches K_∞, the band narrows and damping decreases, as shown by Curve A in comparison with Curve B in Fig. 2. When K_s exceeds K_∞, negative damping occurs, and the bearing becomes unstable. Therefore, the bearing must be carefully designed to exploit this limited damping. The high-frequency stiffness (K_∞) is the primary constraint on the dynamic stiffness and damping of the bearing because K_∞ is limited by the film thickness (H), supply pressure (P_s), bearing area (A_t), recess volume (V_r), and load (W).

An effective way of using its frequency limited damping is to tune the bearing to damp the primary resonance of the machine of which it is a part. A bearing's dynamic stiffness is tuned by shifting it in frequency, as shown by curves A and C in Fig. 2. For purposes of bearing design, this resonance is modeled by an equivalent single degree of freedom (SDOF) system analogous to a lumped mass (M) riding on the bearing. The transfer function relating the motion of the bearing (h(s)) to a dynamic excitation force (f(s)) acting on the mass is

$$\frac{-h(s)}{f(s)} = \frac{1}{Ms^2+K_b(s)} \quad . \tag{3}$$

The natural frequency (ω_n) and the damping ratio (ζ) of the system's resonance are obtained from the complex roots (poles) of the transfer function's denominator. The equivalent SDOF model (Eqn. 3) can also incorporate springs in series and in parallel with the bearing to represent structural stiffnesses affecting the first vibration mode of the machine.

To study the influence of the bearing parameters (K_s, τ_1, τ_2) on ω_n and ζ, Eqns. 1 and 2 are represented in terms of dimensionless parameters by substituting

$$\bar{s} \triangleq \tau_1 s \quad ; \quad \bar{\kappa} \triangleq \frac{K_\infty \tau_1^2}{M} \quad \text{and} \quad \bar{\alpha} \triangleq \frac{K_\infty}{K_s} = \frac{\tau_1}{\tau_2} \quad . \tag{4}$$

The result is

$$K_\infty \frac{-h(s)}{f(s)} = \frac{\bar{\kappa}(\bar{\alpha}+\bar{s})}{\bar{s}^2(\bar{\alpha}+\bar{s}) + \bar{\kappa}(1+\bar{s})} \quad . \tag{5}$$

The definitions of $\bar{\alpha}$, $\bar{\kappa}$, and K_∞ can also be modified to represent the effect of any additional springs in the SDOF model[1]. Because K_∞ is constrained, only the stiffness ratio ($\bar{\alpha}$) and the parameter $\bar{\kappa}$ are free to be tuned. Therefore, an increase in $\bar{\alpha}$ implies that the static stiffness (K_s) must decrease. In Ref. 1, the bearing is shown to provide maximum damping to the system resonance when $\bar{\kappa} = \bar{\alpha}^{-1.5}$. The damping ratio (ζ) for this condition of maximum damping is plotted as a function of $\bar{\alpha}$ in Fig. 3. Note that critical damping ($\zeta = 1$) is approached as $\bar{\alpha} \to 6$ and that damping goes to zero as $\bar{\alpha} \to 1$. The

peak value of the transfer function in Eqn. 5 (denoted by $1/K_{peak}$) occurs at the damped natural frequency (ω_n) and is a function of the damping ratio. The ratio K_{peak}/K_s is also plotted in Fig. 3 as another indication of damping. The natural frequency (ω_n) is plotted in dimensionless terms using both K_s and K_∞ in Fig. 3. Note that if K_∞ is held constant as $\bar{\alpha}$ increases, the natural frequency will decrease because of the accompanying decrease in K_s.

The plots in Fig. 3 illustrate the significance of the bearing's dynamic stiffness on the overall dynamic behavior of the machine-bearing system. The choice of $\bar{\alpha}$ must be carefully considered because of the compromise between damping and K_s (or ω_n). An $\bar{\alpha}$ of 2 is usually a good compromise between the two because it does not have a large static stiffness penalty and because the damping ratio exceeds 20% of critical, which is much greater than the 1-3% damping inherent in most structures. The minimum practical $\bar{\alpha}$ is near 1.5 because of its proximity to the stability limit $\bar{\alpha} = 1$. Also, the additional damping obtained for $\bar{\alpha} > 4$ does not produce a substantial improvement in the system performance. In particular, the peak response ($1/K_{peak}$) reaches a minimum at $\bar{\alpha} = 3$ when K_∞ is held fixed. This is illustrated by scaling the K_{peak} curve in Fig. 3 by $1/\bar{\alpha}$. As a result, the design procedure presented in the next section considers only three choices for $\bar{\alpha}$ (1.5, 2.0, and 4.0).

Another consideration in the selection of $\bar{\alpha}$ is the range of loads (W) and the equivalent SDOF masses (M) under which the bearing must operate. Because K_∞ decreases and K_s increases when the load (W) is reduced below the design value for a bearing[1], $\bar{\alpha}$ will decrease dramatically. As a result, a large $\bar{\alpha}$ should be selected when the range of expected loading is large, thereby ensuring stability under all operating conditions. A change in M does not influence $\bar{\alpha}$, but it will detune $\bar{\kappa}$ from the point of maximum damping. Effectively, a change in M moves the resonant frequency away from the maximum damping frequency of the bearing. To illustate this effect, consider the parameter

$$\bar{c} \triangleq \frac{\bar{\kappa}}{\bar{\alpha}^{1.5}} . \tag{6}$$

At the point of maximum damping, $\bar{c} = 1$. Figure 4 illustrates the influence of other values of $\bar{c}$ corresponding to two- and four-fold variations of M, on the

natural frequency and damping ratio of the system. The curves in Fig. 4a can also be expressed in terms of K_∞, similar to Fig. 3, by scaling them by $\bar{\alpha}^{-0.5}$. Figure 4 illustrates the penalty in lost damping for $\bar{c} \neq 1$ and the increase in natural frequency as $\bar{c}$ increases. For example, a four-fold increase in M will decrease ζ by 30% when $\bar{\alpha} = 2$. Note that a large $\bar{\alpha}$ will provide damping over a wider range of $\bar{c}$ than a small $\bar{\alpha}$, making a large $\bar{\alpha}$ a better choice if M varies widely.

DESIGN PROCEDURE FOR THE ABC BEARING

The purpose of this design procedure is to identify the bearing parameters: μ, R, T, k, R_o, R_i, C_dA_o, H, V_r, N, P_a, and P_s that satisfy the design requirements of a particular application and maximize K_∞. There are many requirements that can be placed on a bearing design, and the most stringent requirement will vary from one application to another. As a consequence, the design procedure must be iterative. An initial choice of bearing parameters may satisfy one requirement, but will probably violate another, thus requiring a revised parameter selection or a relaxed requirement. In addition, there are constraints placed on the parameter selection by the modeling assumptions discussed previously, which are not under the discretion of the designer. The definition of design requirements is an important part of the bearing design process. However, a design problem that is physically impossible to solve can be easily posed. As a result, the initial design requirements will most likely have to be modified in the design process.

The key feature of this design method is the use of Figs. 5, 6, and 7, which correspond to the three design values for $\bar{\alpha}$ (1.5, 2.0, and 4.0) and the three different numbers of interior grooves (N = 0, 3, and 6). In the three figures, the dimensionless static stiffness (K_s), the radius ratio (R_i/R_o), and the recess pressure ratio (P_r/P_s) are plotted as functions of the bearing design parameter ($\Psi = \mu^2 A_t^3/P_s M H^5$) for five values of $\bar{V}_r = V_r/HA_t$. The shape of the curves changes dramatically as the number of interior grooves increases. This behavior is due to the predominance of squeeze film damping in the interior region over the viscous flow damping in the perimeter region when no interior grooves are present. When six interior grooves[3] are present,

viscous flow damping dominates the squeeze film damping in the interior because the interior region responds seven times faster to a change in film thickness than if no interior grooves were present. The large separation between the plots in Figs. 5, 6, and 7 for different numbers of grooves is due to the use of long radial grooves (0.2 to 1.0 R_i). If shorter grooves were also used, intermediate sets of curves could be generated, but they are often not required in practice. Also note from the curves of Figs. 5-7 that bearings with recess volumes less than $0.1HA_t$ are almost equivalent to bearings with no grooves, and that a bearing with a large $\bar{\alpha}$ and a large R_i/R_o is less sensitive to $\bar{V}_r$ than bearings with small $\bar{\alpha}$ and small R_i/R_o.

For given values of Ψ, $\bar{\alpha}$, and $\bar{V}_r$, the stiffness of the bearing is maximized in Figs. 5a, 6a and 7a, if the product P_sA_t/H is maximized. Because these three parameters also appear in Ψ, their selection is coupled. In addition, a large load (W) on the bearing will permit a large P_sA_t and consequently a high stiffness. For this reason, high performance bearings are often implemented in opposed pairs so that a high bearing preload will result, independent of any external load.

An eleven step design procedure for the ABC bearing is presented in Table 1. Variations in this procedure are possible, which may make it more convenient for some applications. In the second column, the Design Requirements are listed in the order they are needed in the design procedure. The other two columns indicate what Parameter Selection and Design Operation is performed at each step and which previously selected Design Parameter needs to be revised if a design requirement or model constraint is not satisfied. In some steps, there is not enough information to initially select a bearing parameter, so it is estimated at first. At a later design step, when more complete information is available, such as values for $\bar{V}_r$ and A_t, the design process must loop back to correct previous estimates. Many iteration loops are possible in the design process; only the most common ones are suggested in the last column of Table 1.

Table 1. ITERATIVE DESIGN PROCEDURE

DESIGN STEP	DESIGN REQUIREMENTS	PARAMETER SELECTION AND DESIGN OPERATIONS	DESIGN PARAMETER TO REVISE (If design requirement is not safisfied)
1.	Ambient pressure P_a and limit on maximum supply pressure (constraint: $P_s > 3P_a$).	Select P_s as large as possible.	
2.	Maximum load W and maximum allowable bearing size.	Select the bearing size (A_t or R_o), (initially $A_t = 1.25W/(P_s-P_a)$, (Figs. 1 and 8).	Increase P_s (Step 1) if A_t is too large.
3.	Range of loads W and masses M, and minimum damping ratio ζ.	Select the stiffness ratio $\bar{\alpha}$ (1.5, 2 or 4) based on the tradeoff between ζ and K_s (Fig. 3) and the range of W and M (Fig 4).	
4.	Gas viscosity μ, minimum allowable film thickness H_m and the mean value of SDOF mass M (Eqn. 3). Constraint on groove number, N = 0, 3 or 6.	Select the number of interior grooves N using the estimate $\Psi = \mu^2 A_t^3/(P_s M H_m^5)$ (Figs. 5b, 6b, 7b).	
5.	Minimum width constraint ($R_o-R_i > 200H$), using H_m initially.	Select the groove radius R_i as large as possible (initially let $\bar{V}_r = 0.1$) (Figs. 5b, 6b, 7b).	If the perimeter region is too narrow, increase A_t (Step 2).
6.	Minimum allowable film thickness.	Determine the film thickness H using R_i and the mean value of M (Figs. 5b, 6b, 7b).	If H is too small, revise R_i or N (Steps 4 & 5). If no suitable R_i or N, decrease P_s (Step 1).
7.		Determine the recess pressure P_r (Figs. 5c, 6c, 7c).	
8.	Maximum applied load and desired stiffness K_s or natural frequency ω_n.	Calculate actual load W (Fig. 8), stiffness K_s (Figs. 5a, 6a, 7a), and frequency ω_n (Fig. 3).	Revise A_t (Step 2), if the calculated load or K_s is not adequate.
9.	Maximum allowable flowrate and the gas properties R and T. Constraint on laminar flow in the film.	Determine the flowrate $\dot{M}$ (Fig. 9).	Reduce H by revising R_i (Step 5), or increasing N (Step 4), if the flowrate is too high.
10.	Allowable groove cross sections and required moment stiffness of the bearing.	Determine the number of flow restrictors and the exact groove volume V_r and the ratio $\bar{V}_r = V_r/HA_t$.	Return to Step 5 to revise $\bar{V}_r$ if necessary.
11.	Minimum allowable orifice size and the specific heat ratio k.	Size the orifice restrictors C_dA_o (Fig. 10).	If the orifices are too small, increase R_i (Step 5).

To maximize bearing stiffness and reduce bearing size, the largest supply pressure permitted by the available facilities should be used (see Design Step 1 of Table 1). (At the Lawrence Livermore National Laboratory, air bearings often use supply pressures of 10 atmospheres). At a minimum, the supply pressure must exceed the modeling limit of $3P_a$. In Step 2, the size of the bearing is estimated from the maximum applied load. If the loading is arbitrary, as with opposed bearings, then the necessary load can be estimated from the desired stiffness by $W = 2HK_s$ or from Fig. 12. Otherwise, the load should be maximized, with the size of the bearing being limited by its space allocation for the particular application. If A_t is larger than desired and the maximum load requirement cannot be reduced, then the supply pressure must be increased (Step 1), which may require an improved gas supply system.

In Step 3, the stiffness ratio $\bar{\alpha}$ must be selected by examining the tradeoff between low frequency stiffness and damping at higher frequency, as discussed in the previous section. Also, a large $\bar{\alpha}$ was shown to benefit system performance if a bearing must operate with a wide range of W and M. These are the most common off-design operating conditions that bearings encounter. The bearing characteristics for off-design conditions are discussed in detail in the following section. In some applications, the bearing must support the weight of a moving element; then W and M are interrelated. In other applications, such as bearings operating in a horizontal plane, W and M are decoupled from one another.

Once $\bar{\alpha}$ is selected, an initial selection of the number of interior grooves (N) can be made in Design Step 4 using either Fig. 5b, 6b or 7b. However, the upper bound of the bearing design parameter ($\Psi = \mu^2 A_t^3 / P_s M H^5$) must first be estimated using the mean value of the expected M and the minimum allowable film thickness. The film thickness (H) is limited by the bearing fabrication process and operational considerations[1]. The number of interior grooves selected should permit the use of a Ψ near this maximum value because maximum bearing stiffness will result when the film thickness is minimized, which corresponds to a large Ψ. Because K_s also increases with R_i/R_o, as shown in Figs. 5a, 6a, and 7a, a large R_i/R_o may produce a higher K_∞ even if Ψ is smaller. For example, an N of 3 will produce a stiffer bearing than a small R_i/R_o and N = 6, even though a larger H is used to obtain the necessary

decrease in Ψ. For R_i/R_o below the region designated on the N = 6 curves in Figs. 5b, 6b, and 7b, a stiffer bearing will result for N = 3 and R_i = $0.98R_o$. However, other design requirements (Steps 9 and 11) or the minimum width constraint for the perimeter region, enforced by the modeling assumptions in Step 5, may prevent the use of large R_i. Before R_i can be selected in Step 5 using Fig. 5b, 6b or 7b, an estimate of the recess volume ratio $\overline{V}_r$ must be made. Because bearing stiffness is diminished for $\overline{V}_r > 0.1$, an initial value of 0.1 is used. Then, for a specified value of N and $\overline{V}_r$, the largest R_i satisfying the width constraint should be selected to maximize bearing stiffness, even if it corresponds to a Ψ below the maximum value.

In Design Step 6, the film thickness is determined from the bearing design parameter (Ψ) that corresponds with the groove radius R_i selected in Step 5. If the selected film thickness is less than that allowed by the design requirement, the selection of R_i in Step 5 and perhaps the selection of N in Step 4 need to be revised so that a smaller Ψ results. If no suitable R_i or N can be found, the supply pressure should be decreased in Step 1 and the bearing area A_t increased in Step 2 to maintain the same load carrying capability. This will allow a larger gap to be used for the same value of Ψ. In the companion figures, Figs. 5c, 6c and 7c, the recess pressure P_r can be determined using the value of Ψ from Figs. 5b, 6b and 7b and the recess volume ratio $\overline{V}_r$.

The design requirements for static stiffness (K_s) and natural frequency (ω_n) are considered in Design Step 8. These requirements are usually determined from an analysis of the overall machine in which the bearings reside. This analysis will ensure that the bearings are not overly stiff relative to the rest of the machine structure. The static stiffness can be determined from Figs. 5a, 6a or 7a, which can then be used to determine the natural frequency (ω_n) of the machine-bearing system using Fig. 3. If these do not meet the design requirements in Step 8, then the load (W) must be increased by increasing the bearing area (A_t) in Step 2. The exact load exerted by the current design can now be determined in Fig. 8, if it does not match the design value, A_t must again be revised in Step 2. All the static bearing characteristics presented in Figs. 8-12 are obtained from standard bearing flow and pressure equations, such as those presented in Gross[2].

The mass flowrate of gas ($\dot{M}$) is determined in Design Step 9 using Fig. 9. If the flowrate exceeds the design requirements or if the modified Reynolds number (Re^*) indicates turbulent flow in the film, the film thickness should be reduced to drop the flowrate. Because of the flowrate's proportionality to H^3, decreasing film thickness is a very effective way of decreasing the flow. However, a larger Ψ must be used to accommodate the smaller H, which also requires a revised R_i selection in Step 5 or a larger N in Step 4. Note that laminar flow is only a requirement of the model used here. ABC bearings are able to operate in the turbulent flow regime, but a more complex model would be required to predict their behavior.

With a known flowrate, the main feed groove can be sized. The model assumes that the perimeter region is supplied uniformly with gas; however, a 1-2% drop in absolute pressure along the groove is reasonable. To obtain a recess volume as close to $V_r = 0.1HA_t$ as possible, the groove cross section should be small and nearly square in shape. Note that a larger groove is required as R_i approaches R_o, because of increased flowrate. However, the design curves of Figs. 5-7 indicate that bearing dynamics become less sensitive to $\bar{V}_r$ as R_i increases. Therefore, the advantages of higher stiffness and load for large R_i outweigh the disadvantages of larger $\bar{V}_r$. The size and shape of the groove may also be restricted by the fabrication method (see Step 10), but the more orifice flow restrictors distributed along the groove, the smaller the main feed groove can be.

In addition, if the bearing is required to have a moment stiffness, the main feed groove can be broken into individually supplied segments. The version of the bearing model used here does not explicitly include the effects of a segmented groove, but if the segment spacing is small, the modeling errors are also small. However, the principle effect of a segmented groove is a decrease in load capacity, which can be partially accounted for in the model by artificially decreasing R_i. Because the radial grooves carry much less flow, they can have a cross-sectional area several times smaller than the main feed groove. The required cross section of the interior grooves can be estimated by assuming that each radial groove must carry the gas displaced by a film of area of $0.7R_i^2/N$ whose thickness is varying by 5% of H at a

frequency of ω_n. Once all the grooves are designed, the actual recess volume can be calculated. If $\bar{V}_r$ exceeds $0.1HA_t$, the design process must return to Step 5 with the revised $\bar{V}_r$.

With the use of Fig. 10 in Design Step 11, the total area of the orifices (A_o) can be determined. In the figure, the orifice area is scaled by a discharge coefficient (C_d) that varies with Reynolds number, pressure difference, and orifice design, but a typical value is 0.8. The discharge coefficient can also be adjusted to account for the mean pressure drop in the grooves, which improves the accuracy of the model. Two penalties occur if many flow restrictors are used. Namely, the orifices are smaller and more difficult to fabricate, and bearing fabrication is more complex and expensive to receive the numerous orifices. If the orifices are too small to reasonably fabricate, the flowrate can be increased to allow larger orifices. One way to do this is to increase R_i in Step 5. After the orifices are sized, the bearing design is complete.

STIFFNESS AND DAMPING OF A SPECIFIED BEARING OPERATING AT OFF-DESIGN CONDITIONS

Once a bearing is designed, it may have to operate at conditions other than those it was designed for. The most common off-design conditions are variations in the applied load (W) and the equivalent SDOF mass (M). In addition, a bearing may deviate from its ideal design geometry due to normal fabrication tolerances. Once a bearing is fabricated, the supply pressure and, to a lesser degree, the orifice area can be modified from the initial design values. Changes to both P_s and C_dA_o can be used to re-tune the bearing to better accommodate changes in M and W. For instance, if P_s increases approximately linearly with W, there will be less impact on the dynamic stiffness of the bearing than if it were constant. The non-iterative procedure presented in Table 2 can be used to determine the static and dynamic characteristics of the bearing at these off-design conditions. It can also be used to fine tune the bearing in its final fabricated state. For instance, the bearing parameters (such as R_i or C_d) that best account for the supply pressure dependence of the measured values of the bearing load, film thickness, and flowrate can be determined from Figs. 8-12. With this

Table 2. PROCEDURE FOR DETERMINING THE STATIC AND DYNAMIC CHARACTERISTICS FOR A SPECIFIC BEARING

STEP NUMBER	ADDITIONAL DESIGN SPECIFICATIONS REQUIRED TO PERFORM THE DETERMINATION	PARAMETER DETERMINATION
Static Characteristics		
1.	Load W, ambient pressure P_a, bearing area A_t and radius ratio R_i/R_o.	Determine the recess pressure P_r (Fig. 8).
2.	Supply pressure P_s, gas properties R and T, the effective orifice area C_dA_o, and recess pressure P_r from Step 2.	Determine the gas flow rate $\dot{M}$ (Fig. 10).
3.	Gas viscosity μ.	Determine the film thickness H (Fig. 11).
4.	Film thickness H from Step 3.	Determine the static stiffness K_s (Fig. 12).
Dynamic Characteristics		
5.	Recess volume V_r.	Calculate the recess volume ratio $\bar{V}_r = V_r/HA_t$.
6.	Recess volume ratio $\bar{V}_r$ from Step 5 and the number of interior grooves N.	Determine the stiffness ratio $\bar{\alpha}$ (Figs. 13a,14a,15a).
7.	Equivalent SDOF mass M and the static stiffness K_s from Step 4.	Determine the dynamic parameter $\bar{c}$ (Figs. 13b,14b,15b).
8.	The stiffness ratio $\bar{\alpha}$ from Step 6 and the dynamic parameter $\bar{c}$ from Step 7.	Determine the SDOF system natural frequency ω_n (Fig. 4a) and the damping ratio ζ (Fig. 4b).

experimentally validated model, the procedure in Table 2 can then be used to predict the dynamic characteristics of the bearing and whether a modified P_s or C_dA_o will improve the dynamic performance of the machine-bearing system.

The procedure in Table 2 is divided into two parts, four steps for determining the static bearing characteristics and four steps for the dynamic characteristics. The second column lists the additional parameter specifications, beyond those used in previous steps, needed to determine a bearing parameter in a particular step. The static characteristics are determined from standard bearing flow equations[2], as illustrated by Figs. 8-12. The recess volume ratio $\overline{V}_r$ calculated in Step 5 of Table 2, is only needed to determine the dynamic characteristics of the bearing. With $\overline{V}_r$ known, the stiffness ratio ($\overline{\alpha}$) can be determined using either Figs. 13a, 14a or 15a, depending on the number of interior grooves. In each figure, $\overline{\alpha}$ is plotted for three values of R_i/R_o (0.8, 0.9, 0.95). For other values of R_i/R_o, the stiffness ratio must be determined by interpolation. Note the weak dependence of $\overline{\alpha}$ on R_i/R_o in the figures and the strong dependence on P_r/P_s. Figures 13a-15a also demonstrate that large recess pressure ratios, much greater than the ratio at maximum K_s ($P_r/P_s \approx 0.7$), are required to achieve significant damping in the ABC bearing. The companion figures, Figs. 13b, 14b, and 15b, can be used similiarly to determine the parameter $\overline{c}$ of Eqn. 6, which is an indication of how far the bearing departs from the maximum damping condition. The last step of the procedure in Table 2 uses $\overline{\alpha}$, $\overline{c}$, and Fig. 4 to determine the damping ratio and natural frequency of the system. This procedure can then be repeated for each new operating condition.

DESIGN EXAMPLE

An example bearing design problem is presented here to illustrate the design procedure and to give a physical example of an ABC bearing. This simple example only shows one of the many ways this design procedure can be utilized. Consider the bearings required to guide a slide for a machine tool along a rectangular guide bar. To restrain horizontal motion, two sets of opposed bearing pairs are needed at each end of the slide. The slide is assumed to be rigid with its first free-free natural frequency exceeding 400 Hz (2500 rad/sec) and a local stiffness at the bearing mounts exceeding

800 MN/m. The bearing pairs are mounted far enough apart that the first resonance of the 1000 Kg slide on the bearings is a horizontal translation. As a result, the effective SDOF mass for tuning one bearing is 250 Kg. Because the slide is excited by dynamic tool forces in the horizontal direction, this vibration mode must be well damped to avoid unstable machining (chatter) and to produce the best possible surface finish on the machined part. Space and fabrication constraints require that the bearings must be less than 60 mm in diameter and the film thickness must exceed 6 μm. The bearing is to be supplied by air at a maximum pressure of 10 atmospheres, and the ambient conditions of the bearing will be near standard temperature and pressure. These initial design specifications for the example problem are listed in Table 3.

Following the design procedure of Table 2, the maximum supply pressure (P_s = 1.012 MN/m^2) is selected in Design Step 1 for the initial bearing design, as indicated in Table 3. Because the bearings are mounted in opposed pairs, their load is not limited by external forces. Consequently, the maximum bearing radius of 30 mm is selected in Step 2 to maximize bearing stiffness. If the resulting bearing load or stiffness calculated in Step 8 exceed the strength or stiffness of the bearing mount, a smaller bearing radius would have to be selected in a later design iteration. For this application, the range of applied loads and slide inertias is small, so a stiffness ratio of 2 is chosen in Step 3 as an acceptable compromise between stiffness and damping.

In Design Step 4 the bearing design parameter Ψ is estimated using the minimum gap thickness of 6 μm. The estimated value of 3.8 indicates in Fig. 6b that a bearing with no interior grooves (N = 0) should be used. Because a large R_i increases stiffness, a thicker air film should be used to reduce Ψ on the N = 0 curves of Fig. 6b. Based on the minimum perimeter region width of $200H_{min}$, the initial groove radius of 28.8 mm is selected in Step 5. For the initial estimate of $\bar{V}_r$ = 0.1, this groove radius corresponds to Ψ = 2.3 and a film thickness of 6.62 μm. The small violation of the perimeter region width constraint can be addressed in subsequent design iterations. From this value of Ψ, the recess pressure is determined in Fig. 6c and the static stiffness from Fig. 6a. The bearing stiffness of 164 MN/m

is well below the mount stiffness, indicating the bearing is not overly stiff for the application. Also, the natural frequency of the slide-bearing system of 948 rad/sec, as determined from Fig. 3, is below the free-free natural frequency of the slide, indicating that the translational vibration mode on the bearings dominates the dynamic response of the slide. The load on the bearing is also calculated in Step 8 using Fig. 8. The load of 2.26 KN is not excessive for a machine tool slide of this type.

The mass flowrate of air through the bearing is now determined using Fig. 9. Even though there is no explicit flowrate constraint, the modified Reynolds number must be determined for the bearing film in Design Step 9. The calculated Re^* of 1.9 exceeds the laminar flow constraint in the perimeter region. Examination of Fig. 9 shows that a groove radius of R_i = 27 mm will reduce the bearing flowrate by more than 60% for the same film thickness. Coupled with the larger width of the perimeter region and a smaller H, Re^* will be reduced by more than a factor of 6, putting the perimeter flow into the laminar regime. Therefore, the second design iteration must return to Step 5 with the revised value of R_i. In Design Step 6, the new value of R_i corresponds to Ψ = 2.85 in Fig. 6b which then corresponds to a film thickness of 6.34 μm. Design Steps 7-9 proceed as before, with the revised flowrate in Step 9 producing an Re^* of 0.26.

In Design Step 10 the main feed groove can be sized. Assuming laminar flow in the groove, three equally spaced orifices are required to supply a square, 0.3 x 0.3 mm, groove so that a pressure drop of less than $0.01P_r$ occurs along the groove. The resulting recess groove volume of 15.3 mm^3 corresponds to a volume ratio $\bar{V}_r$ = 0.85. This value exceeds the initial estimate of 0.1. Therefore, the next design iteration must return to Design Step 5 with a revised $\bar{V}_r$. This final iteration is very similar to the second, with only a small increase of Ψ to 3.0. The predicted flowrate in Step 9 is slightly less than the previous iteration so the groove design can remain the same. In the last Design Step, the orifice size can be selected using Fig. 11. The total effective orifice area required is C_dA_o = 0.283 mm^2. For three orifices and a C_d = 0.8, the required orifice diameter is 0.39 mm, which is a size that can be easily fabricated.

With the selection of the orifices, the bearing is completely specified. Reference 1 discusses a bearing with similar specifications that was built and tested. The test results indicated that the frequency-dependent stiffness and damping agreed well with that predicted by the dynamic model and it demonstrated the practicality of an ABC bearing.

Table 3. DESIGN EXAMPLE

Initial Parameter Specifications:

Gas Properties (Air at standard conditions)

$\mu = 1.81 \times 10^{-5}$ N-sec/m^2

$k = 1.4$

$R = 287$ N-m/Kg-°K

$T = 293$°K

$P_a = 0.1012$ MN/m^2

$R_{o,max} = 30$mm

$H_{min} = 6\mu m$

$M = 250$Kg

DESIGN STEP	DESIGN PARAMETER	INITIAL DESIGN	SECOND ITERATION	FINAL DESIGN
1.	P_s	1.012 MN/m^2	1.012 MN/m^2	1.012 MN/m^2
2.	R_o	30 mm	30 mm	30 mm
3.	$\bar{\alpha}$	2	2	2
4.	N	0	0	0
5.	est. $\bar{V}_r$	0.1	0.1	0.85
	R_i	28.8 mm	27 mm	27 mm
6.	H	6.62 μm	6.34 μm	6.28 μm
7.	P_r	0.926 MN/m^2	0.930 MN/m^2	0.931 MN/m^2
8.	W	2.26 KN	2.17 KN	2.18 KN
	K_s	164 MN/m	167 MN/m	164 MN/m
	ω_n	948 rad/sec	957 rad/sec	948 rad/sec
9.	$\dot{M}$	1.11 g/sec	0.384 g/sec	0.373 g/sec
10.	V_r	--------	15.3 mm^3	15.3 mm^3
11.	C_dA_o	--------	--------	0.283 mm^2

CONCLUSIONS

The ABC bearing presented here is readily tuned to the dynamics of the supporting structure and has high stiffness and damping because of the squeeze film in its large interior region. The model of the bearing used here represents its dynamic stiffness as a single pole and zero transfer function. In the suggested design procedure the frequency limited damping, modeled by the pole and zero, is tuned to provide maximum damping at the natural frequency of the machine-bearing system. The damping ratio of a typical ABC bearing design can exceed 20%, which is more than 10 times that commonly achieved when only the stability, static stiffness, and load capacity of a bearing are considered. However, the resonance of the machine-bearing system becomes less damped when the applied load or the inertia of the attached machine deviate from design conditions.

A design procedure is suggested here in which the design requirements for a particular application can be iteratively evaluated and revised. The design tradeoffs necessary to maximize bearing stiffness and damping, under a given set of design constraints, is shown. A key feature of the design technique is the tuning of dynamic stiffness through adjustment of the radius of the main feed groove of the bearing and selection of the number of its interior, radial grooves.

This design method emphasizes the tuning of damping and maximizing the high frequency stiffness of a bearing of limited size. Typically, the ABC bearing will use a higher supply pressure, have a smaller film thickness, and have a larger main-feed groove radius than a bearing designed with common methodology. To achieve the high damping, the recess to supply pressure ratios used here exceed 0.8, which is well above the pressure ratio that maximizes the static stiffness of a bearing. Because of the large interior region, the dynamic stiffness of ABC bearings is not as sensitive to the volume of the recess grooves, thus allowing higher flowrates and groove radii than is typical. The large interior region also increases the load capacity of the bearing compared with other bearings of comparable size. Finally, the ABC bearing is practical and is implemented in operating machinery.

ACKNOWLEDGMENTS

The authors kindly thank Shirley Rock and Patricia Flowers for their assistance in the preparation of this document.

AUSPICES

Work performed under the auspices of the U.S. Department of Energy by the Lawrence Livermore National Laboratory under contract number W-7405-ENG-48.

REFERENCES

1. J. W. Roblee, Design of Externally Pressurized Gas Bearings for Dynamic Applications, Ph.D Thesis, University of California; Berkeley, CA; April, 1985.

2. W. A. Gross, Gas Film Lubrication; John Wiley and Sons, Inc.; New York, NY; 1962.

3. J. W. Roblee and C. D. Mote, Jr., "Vibration Damping in Externally Pressurized Gas Bearings," Lawrence Livermore National Laboratory; Livermore, CA; October, 1986; UCRL-93600 Preprint, Presented at the International Conference of Vibration Problems in Engineering; Xi'an, China; June, 1986.

P86-053
9/5/86

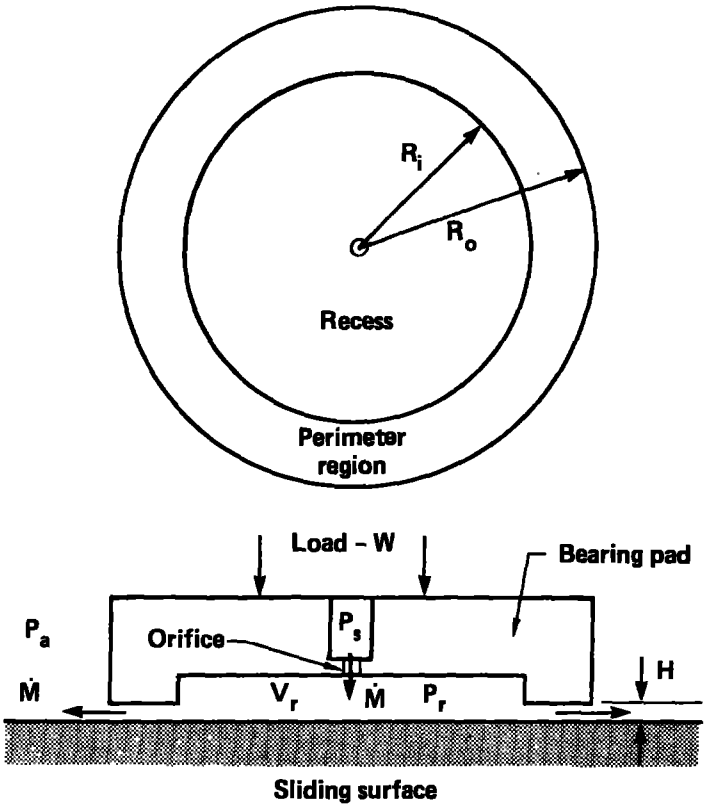

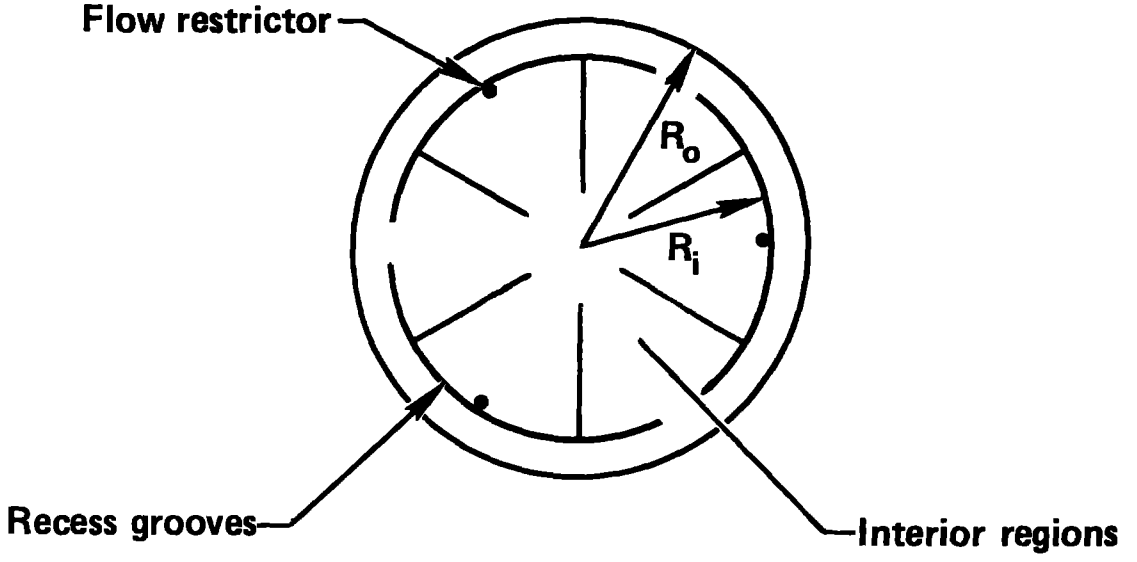

Fig. 1a,b. Geometry and gas flow paths of flat, circular, thrust bearings.

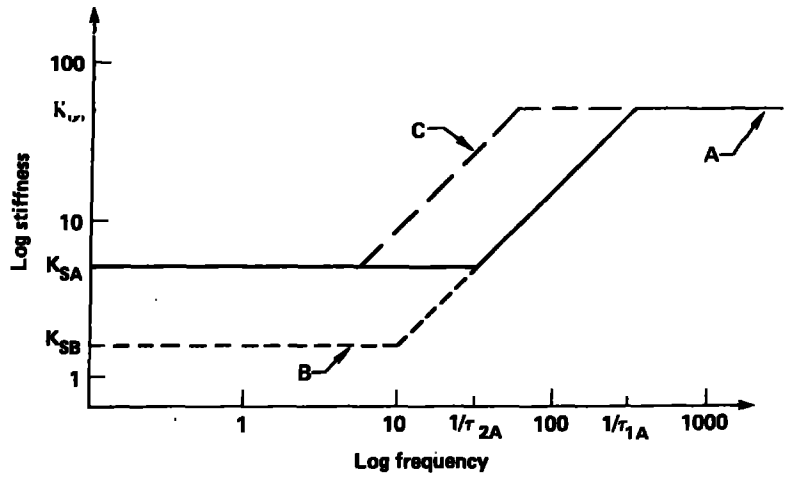

Fig. 2. Three possible dynamic stiffness amplitudes for a gas bearing.

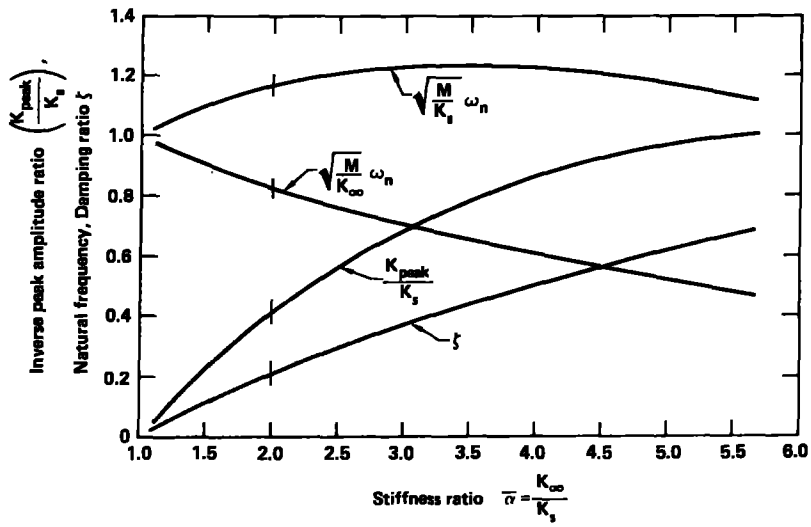

Fig. 3. The influence of the bearing stiffness ratio on a SDOF bearing system dynamics tuned for maximum damping.

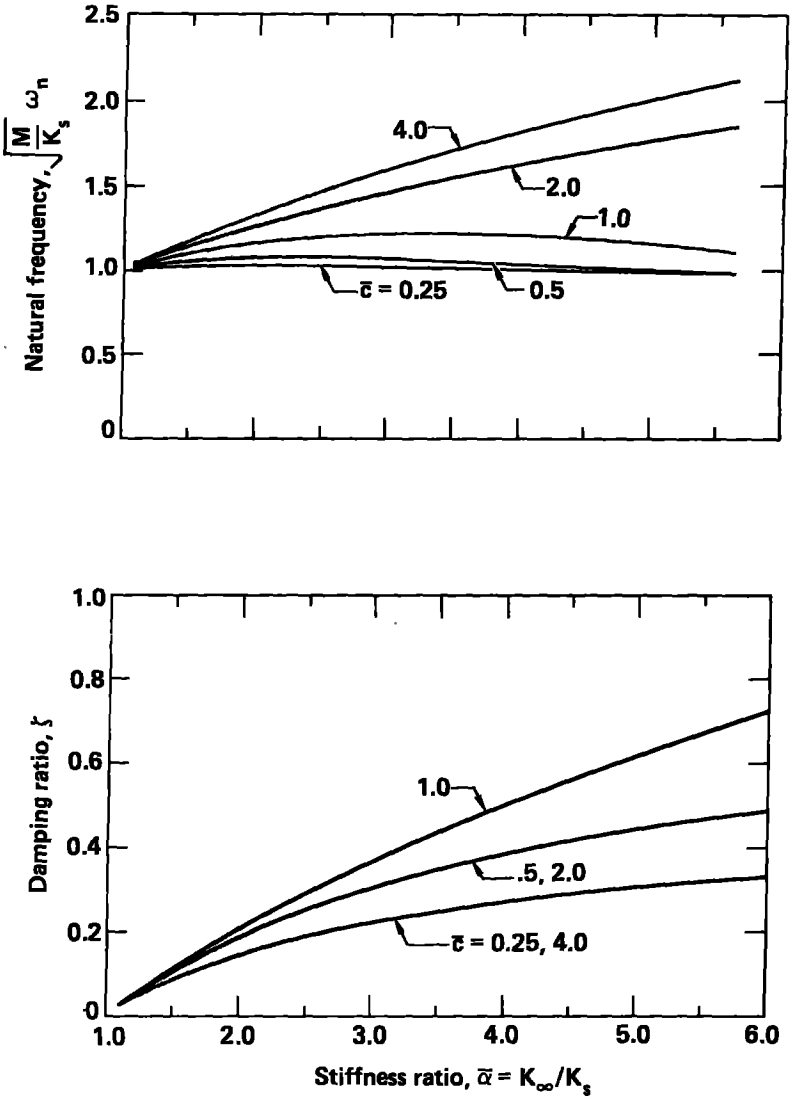

Fig. 4a,b. The influence of bearing stiffness shifted in frequency from the maximum damping frequency (when $\bar{c}$ = 1) on the SDOF system dynamics.

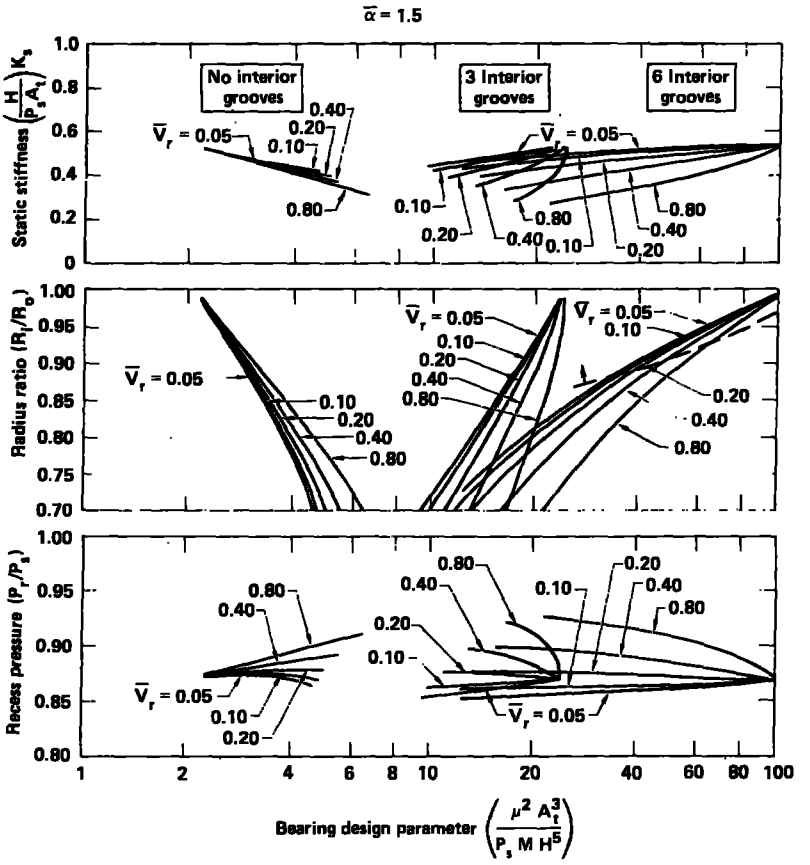

Fig. 5a,b,c. Bearing design charts for a stiffness ratio $\bar{\alpha}$ = 1.5.

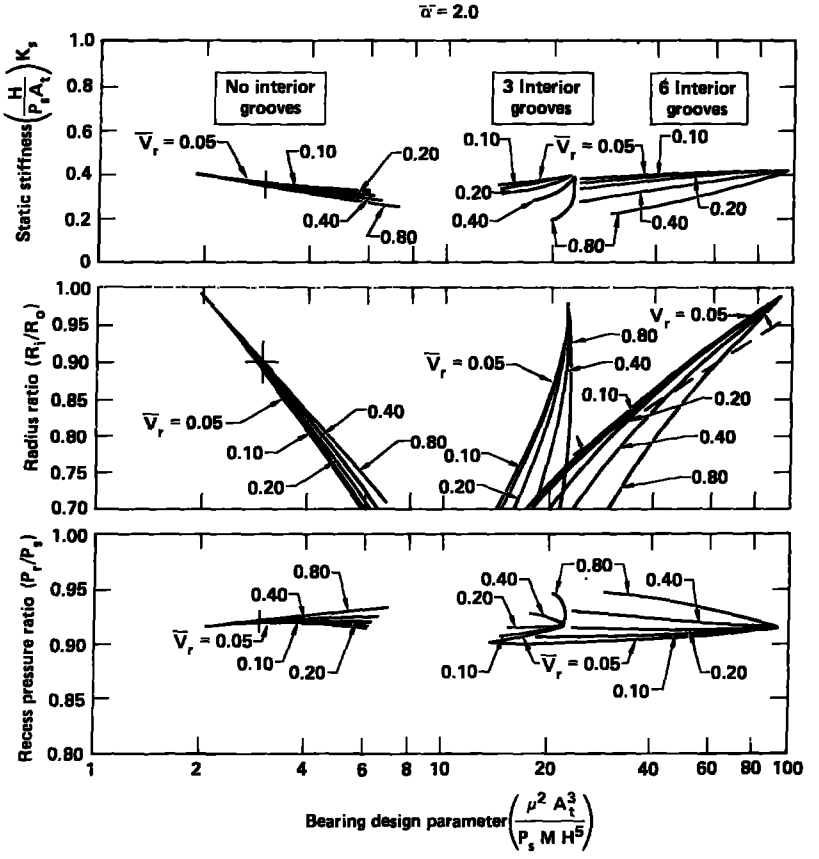

Fig. 6a,b,c. Bearing design charts for a stiffness ratio $\bar{\alpha}$ = 2.0.

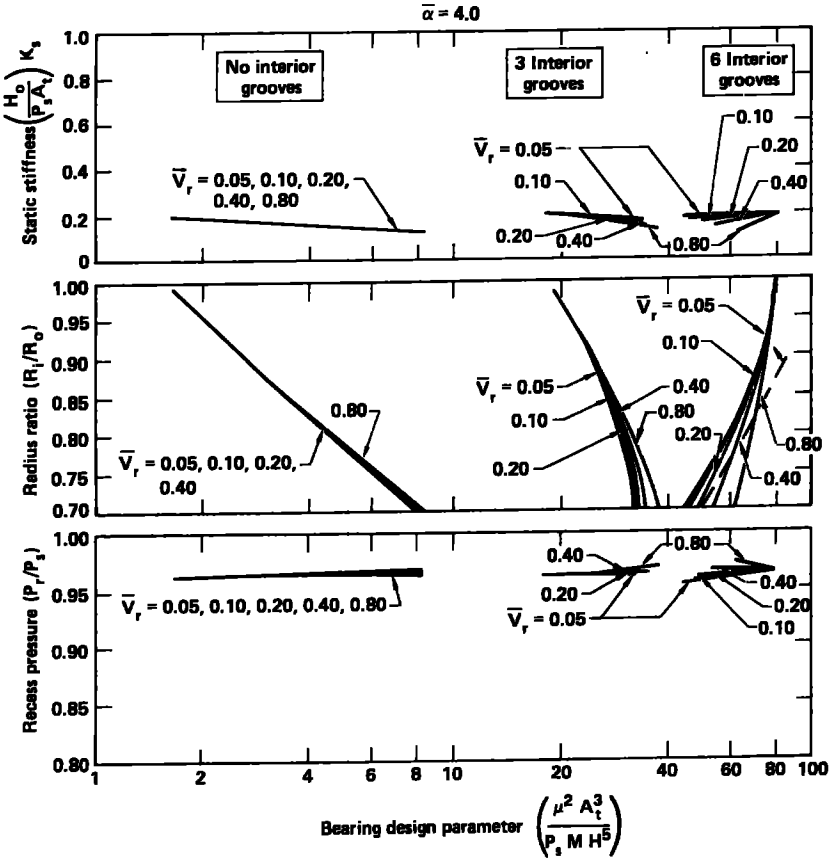

Fig. 7a,b,c. Bearing design charts for a stiffness ratio $\bar{\alpha}$ = 4.0.

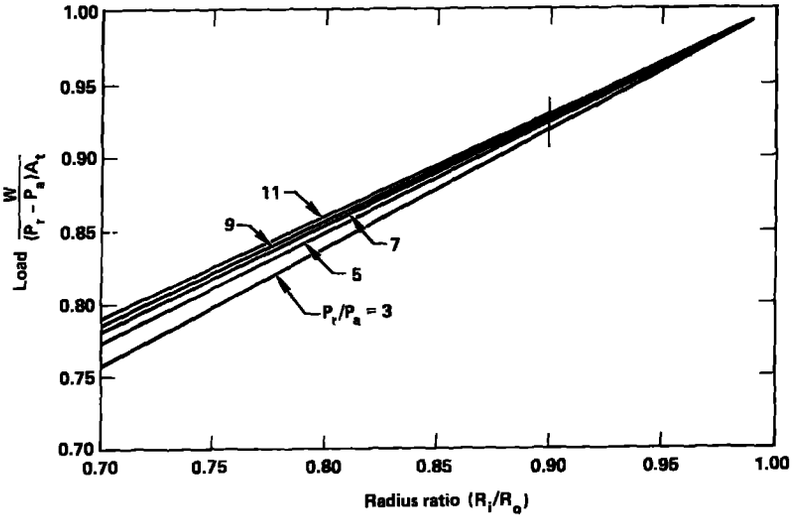

Fig. 8. Bearing load for different recess pressures P_r.

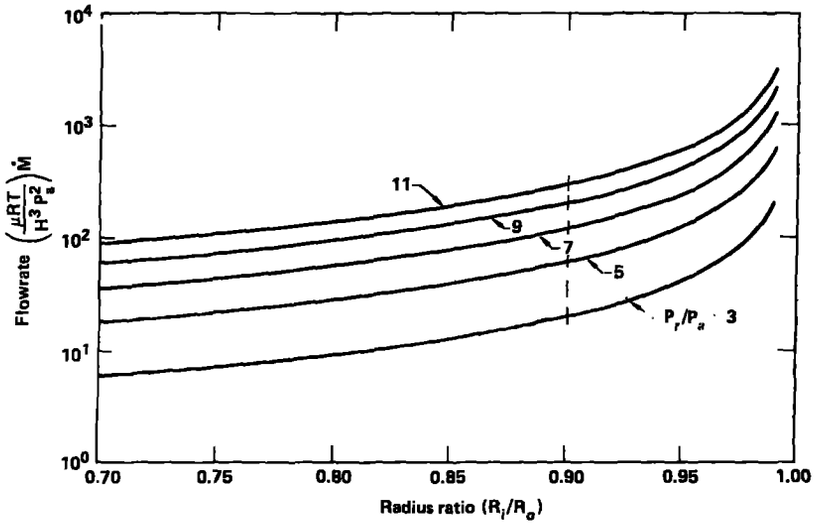

Fig. 9. Gas flowrate through a bearing gap of height H and recess pressure P_r.

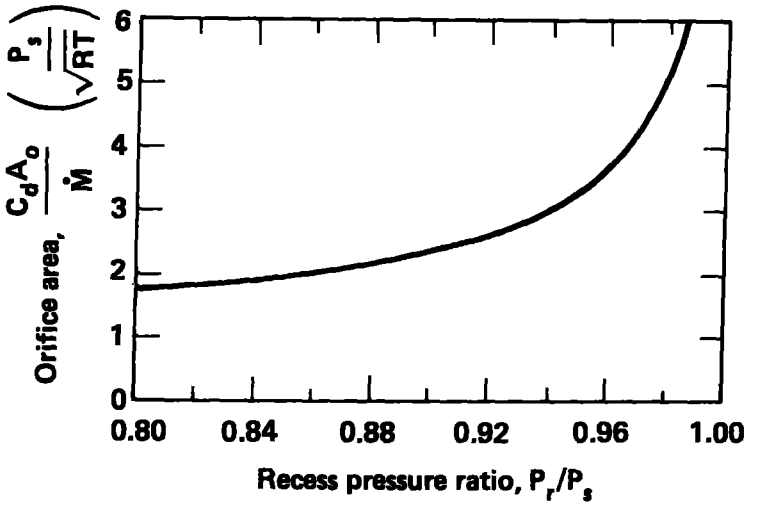

Fig. 10. The orifice area A_o required for a given recess pressure ratio at a flowrate $\dot{M}$.

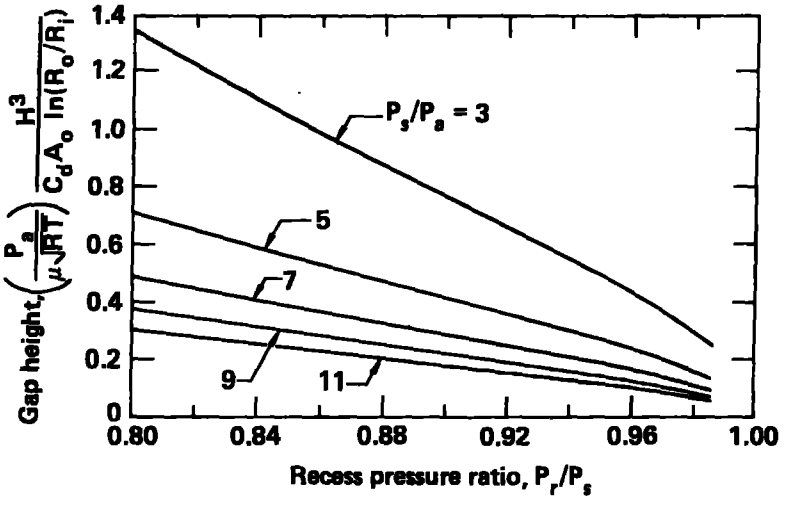

Fig. 11. Gap height of a specified bearing at different supply and recess pressures (P_s and P_r).

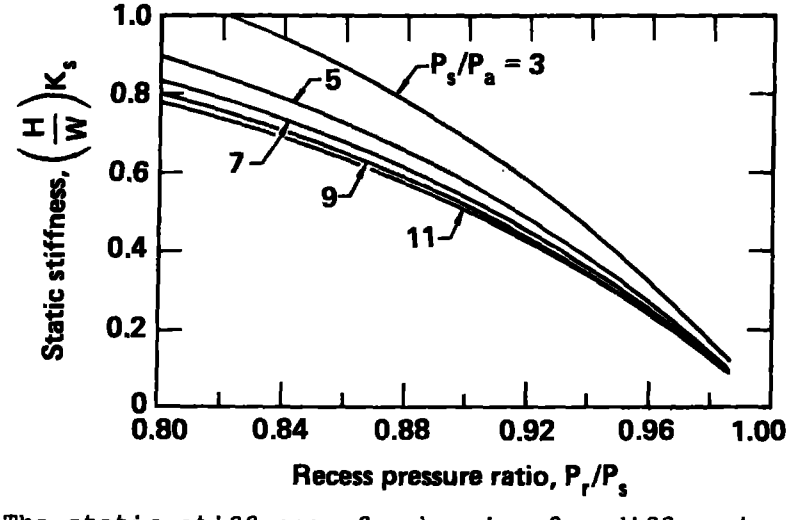

Fig. 12. The static stiffness of a bearing for different supply and recess pressures (P_r and P_s).

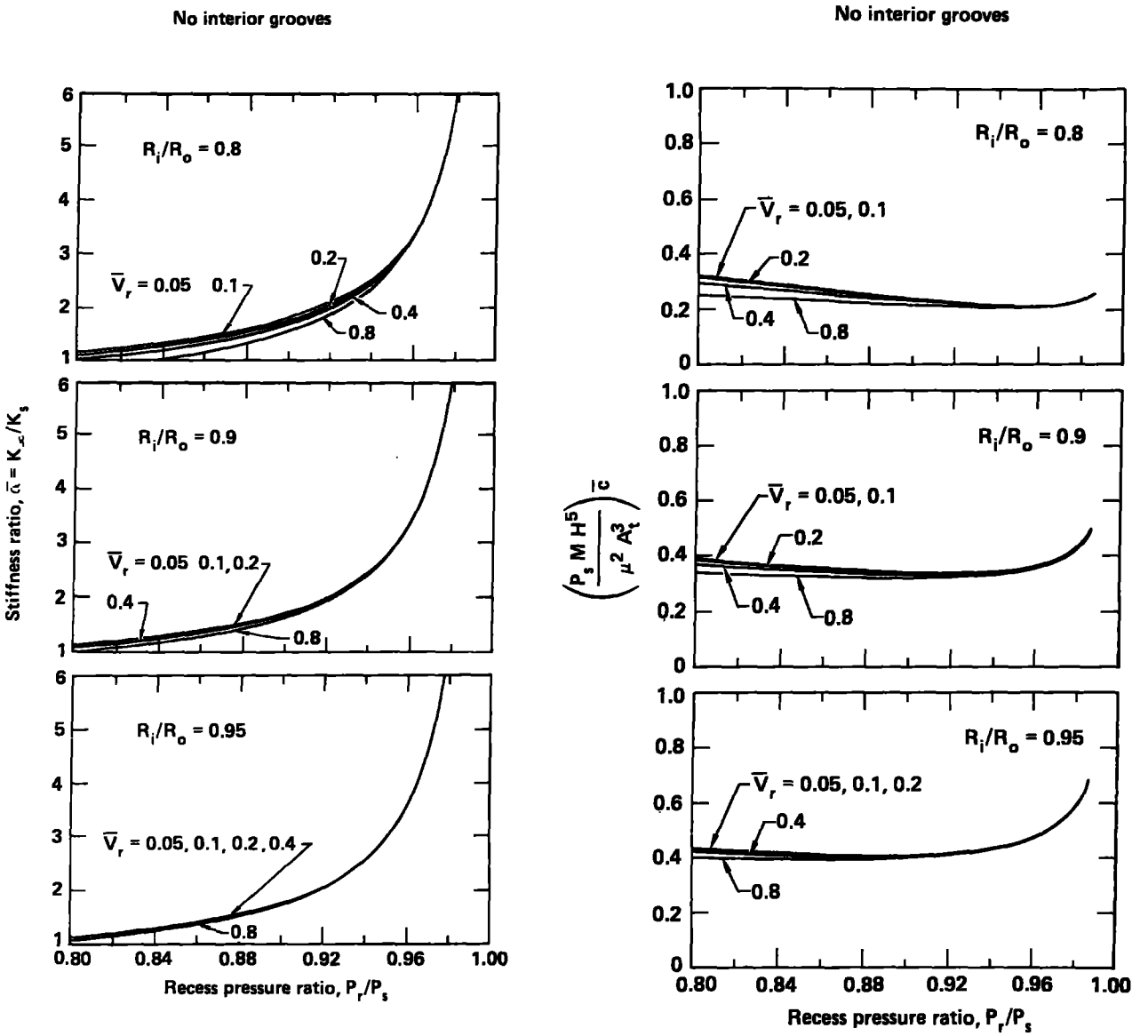

Fig. 13a,b. Charts to determine the bearing dynamic parameters $\bar{\alpha}$ and $\bar{c}$ for a bearing with no interior grooves and operating at recess pressure P_r.

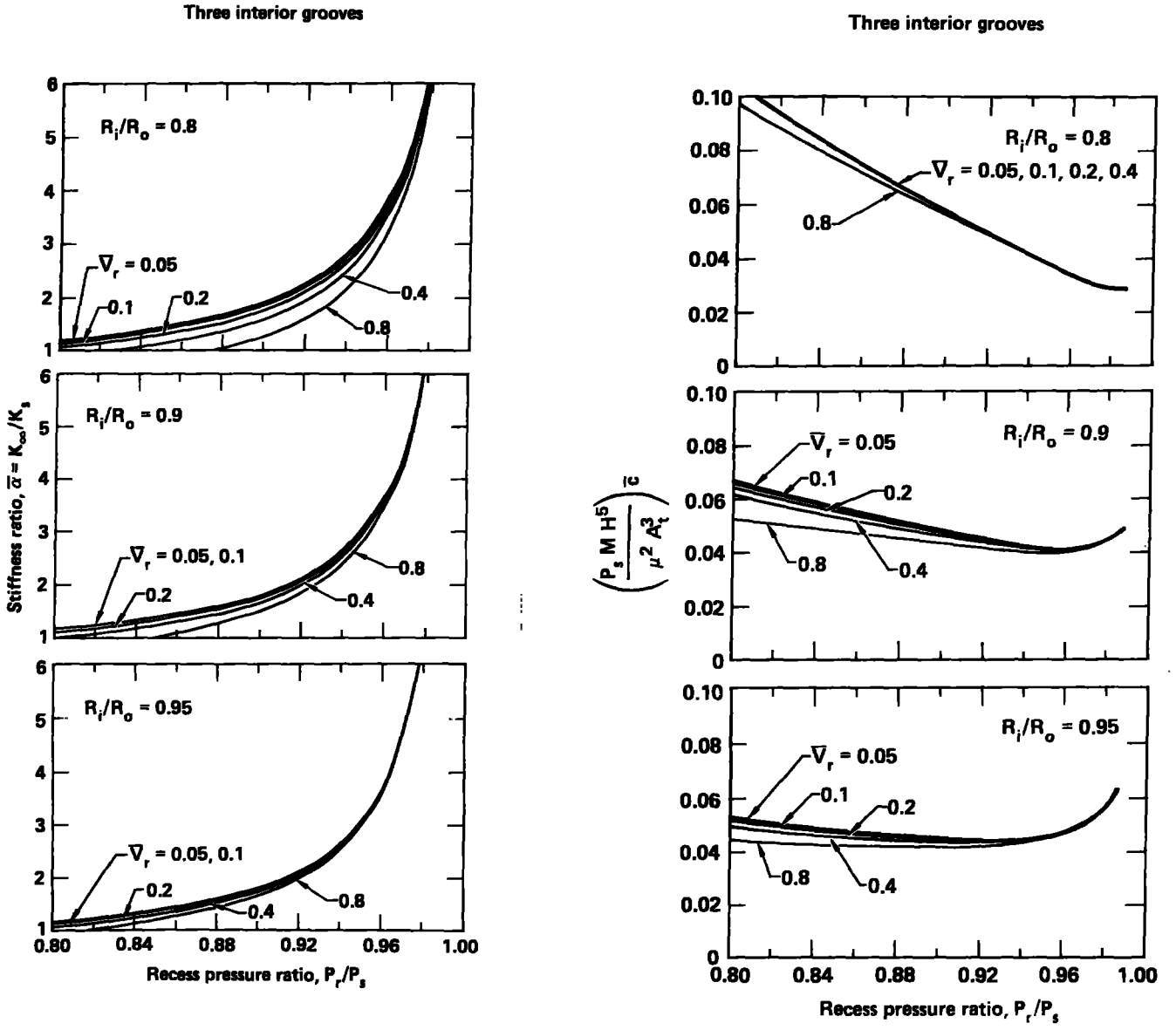

Fig. 14a,b. Charts to determine the bearing dynamic parameters $\bar{\alpha}$ and $\bar{c}$ for a bearing with three interior grooves and operating at recess pressure P_r.

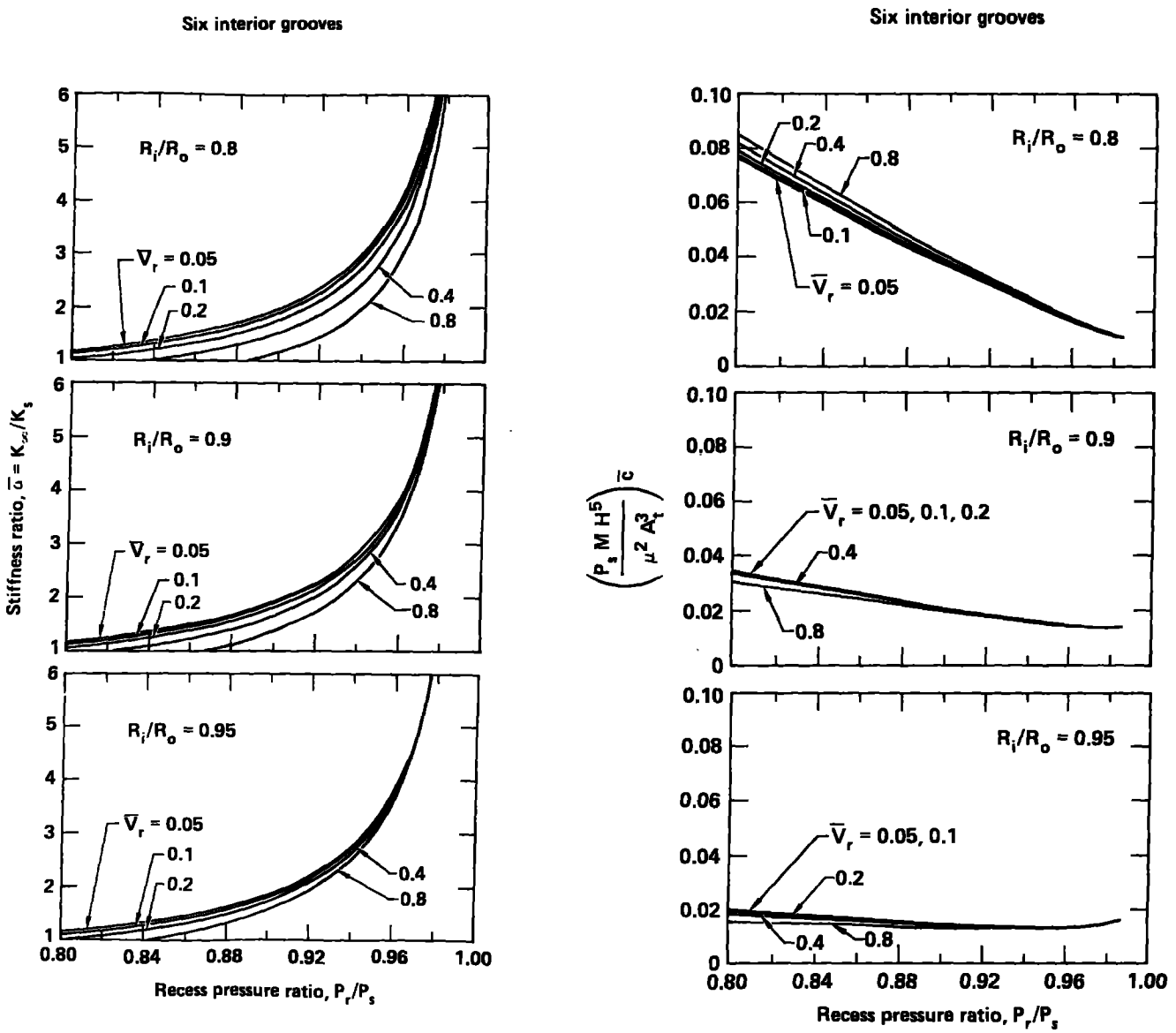

Fig. 15a,b. Charts to determine the bearing dynamic parameters $\bar{\alpha}$ and $\bar{c}$ for a bearing with six interior grooves and operating at recess pressure P_r.